Quantitatively Monitoring of Seasonal Frozen Ground Freeze-thaw Cycle Using Ambient Seismic Noise Data

Hui Liu[1], Jing Li[1,2*] Rong Hu[1] and Benxin Chi[3]

[1] College of Geo-Exploration Science and Technology, Jilin University, Changchun, 130026, China

[2] Key Laboratory of Applied Geophysics, Changchun 130026, China

[3] State Key Laboratory of Geodesy and Earth's Dynamics, Innovation Academy of Precision Measurement Technology and Science, Chinese Academy of Sciences, Wuhan, China

Corresponding author: Jing Li (inter.lijing@gmail.com)

Key Points:

We proposed integrating ambient noise seismic processing framework to quantitatively monitor the seasonal frozen ground freeze-thaw cycle.

The surface-wave dispersion curve variations (dc/c) strongly correlate negatively with air temperature and soil moisture content.

The horizontal-to-vertical spectral ratio (HVSR) and seismic attenuation show highly consistent changes to the freeze-thaw processes.

Abstract

Seasonal frozen ground freeze-thaw cycles in cold regions are an essential indicator of climate change, infrastructure, and ecosystems in the near-surface critical zone (CZ). As a non-invasive geophysical method, the ambient noise seismic method estimates the relative velocity variations (dv/v) based on coda waves or ballistic waves, providing new insights into the seasonal frozen ground changes in the soil properties and hydrology data, such as soil moisture content (SMC), temperature, and groundwater level. Due to the dv/v lack of accurate depth information and average over tens of days at low frequencies, it is challenging to provide the needed temporal-spatial resolution for the micrometer-level frozen ground variation. In this work, we combine the 1D linear three-component seismic array and hydrological sensor to conduct seasonal frozen ground freeze-thaw monitoring experiments. Besides the conventional dv/v information, we calculate surface-wave (SW) dispersion curve variations (dc/c), which are more sensitive to SMC and can characterize the daily air temperature variations. Meanwhile, the horizontal-to-vertical spectral ratio (HVSR) amplitude and seismic attenuation also show highly consistent changes to the freeze-thaw processes. This work demonstrates that the different ambient noise seismic information (dc/c, HVSR, and attenuation) provide robust observations for hydrogeological monitoring, such as air temperature, SMC, and groundwater level changes during seasonal freeze-thaw processes.

Plain Language Summary

In cold parts of the world, the ground freezes and thaws as seasons change. This natural process significantly affects both the environment and human-made structures. Understanding these freeze-thaw cycles is crucial, but observing them without disturbing the ground has been challenging. Our study used ambient seismic noise data to monitor ground physical properties during the freeze and thaw cycle. The approach involves analyzing changes in the surface-wave dispersion curves from linear array seismic data, which is more sensitive to changes in soil moisture and daily temperature variations than traditional methods based on coda wave or ballistic wave velocity variations (dv/v). Additionally, we integrate the spectrum of ambient noise and attenuation to understand the freeze-thaw cycles better. Our findings highlight the effectiveness of this approach in environmental monitoring, offering an improved method for predicting and managing the impacts of freeze-thaw cycles on ecosystems and infrastructure in cold climates.

1. Introduction

Seasonal freezing and thawing occur over more than half of the land area of the Northern Hemisphere (Miao et al., 2019). Several factors influence its formation and degradation, including climate change, topography, soil, and vegetation type (Zhang et al., 1997; Jorgenson et al., 2001; Nelson, 2003; Frauenfeld & Zhang, 2011). The formation of seasonally frozen ground can affect soil physical properties such as soil structure, porosity, and moisture, which in turn affect vegetation growth and soil hydrological processes (Niu et al., 2011; Walvoord & Kurylyk, 2016; Vecellio et al., 2019). In recent decades, the degradation of frozen ground has significantly affected local hydrology, ecosystems, and engineering infrastructure as soil temperatures have increased in response to global warming (Cheng & Wu, 2007; Harris et al., 2009; Green et al., 2019). Therefore, monitoring and understanding seasonal ground freeze-thaw processes and spatiotemporal evolution patterns is particularly important.

However, dynamic monitoring of seasonal frozen ground freeze-thaw processes in the field is limited by monitoring conditions in cold regions and cost, making it difficult to obtain long-term soil monitoring information (Qin et al., 2018). Directly monitoring frozen ground is possible through borehole temperature logging, but geological conditions and cost constraints limit its widespread use. Surface geophysical methods such as electrical resistivity tomography (ERT) and active source seismic (Hornum et al., 2021; Stemland et al., 2021; Scandroglio et al., 2021) can distinguish between frozen and non-frozen areas but require prolonged and repeated measurements to achieve temporal resolution, acquiring in environmentally challenging regions challenging and laborious (Mollaret et al., 2019).

To overcome these problems, passive source seismic methods have been rapidly developed in recent years to monitor seasonal variations in relative velocities variations (dv/v) during the freeze-thaw of the frozen ground using cross-correlation functions of ambient noise seismic records (Wang et al., 2017; Miao et al., 2019; Albaric et al., 2021; Steinmann et al., 2022; James et al., 2019). Lindner et al. (2021) found seasonal variations in seismic velocities and long-term velocity decreases due to seasonal freeze-thaw cycles and multi-year permafrost degradation over 15 years by calculating dv/v obtained from cross-correlations at a single station at Mt. Zugspitze, Germany. They also compared the results with meteorological data, suggesting that seasonal freeze-thaw cycles and permafrost degradation contribute to these velocity variations. In addition, Cheng et al. (2022) utilize the distributed acoustic sensing (DAS) approach to monitor permafrost degradation seismically during a controlled heating experiment. Besides, the horizontal-to-vertical spectral ratio (HVSR) method (Nakamura et al., 1989) typically uses resonant frequencies to estimate the depth of the basement and reveals freeze-thaw changes by HVSR amplitude information (Kula et al., 2018; Steinmann et al., 2022).

However, the dv/v lacks accurate depth information and averages over tens of days at low frequencies. It is challenging to provide the needed temporal and spatial resolution quantitatively in the previous studies (Miao et al., 2019; James et al., 2019; Cheng et al., 2022; Qin et al., 2022). The observed variations in the surface-wave dispersion curve (dc/c) at most sensitive frequencies consistently correlate with soil properties. They can be forward modeled given a subsurface model with reasonable accuracy and spatial resolution (Sobolevskaia et al., 2021). In addition to spatial velocity variations, seismic data includes other information, such as resonance frequency and attenuation (peak frequency information). Using different information to compare and verify is of great significance for improving the reliability of results.

In this work, we explore the utility of ambient noise seismic techniques for monitoring site scale seasonal frozen freeze-thaw cycle physical proprieties, such as air/soil temperature, soil moisture content (SMC), and groundwater level depth. The field data at the hydrological observation site demonstrate that the estimated time-varying dc/c and peak frequency of seismic data have a strong negative correlation with temperature and SMC. There is perfect consistency between dc/c and peak frequency with changes in air temperature. The amplitude of HVSR can indicate the current lowest temperature, while there is a certain lag in dc/c and peak frequency, which is more consistent with the cumulative temperature. The different seismic data information suggests that ambient noise seismic technology is promising for monitoring seasonal permafrost freeze-thaw processes.

2. Experiment and Data

The experimental site of frozen ground monitoring is located at the hydrological observation site of Jilin University, Northeast China, from October 2021 to June 2022 (Figures 1a and 1b). The annual temperature difference is within the range of -20 to 30 C. We deployed a 1-D linear array with 12 three-component seismic nodes to record the urban environmental noise signals, with a node spacing of 5 m and a temporal sampling rate of 500 Hz. Meanwhile, we used a real-time weather station to record the air temperature, rainfall, and atmospheric pressure. The HOBO water level logger records the groundwater level. The TRIME-PICO sensors time domain reflectometry (TDR) is arranged at 0, 10, 20, 30, 40, 50, 65, 80, 100, 125, 150, 170, 185, 200, 215, 230, 250, 275, and 300 cm depth to record changes in soil temperature and SMC during freeze-thaw cycles.

Following the ambient seismic noise data process workflow (Bensen et al., 2007; Schimmel & Gallart., 2007), we calculate the noise cross-correlation function (NCF) in Figure 1c. The corresponding surface-wave dispersion curve shows continuous fundamental and high modes in the frequency range of 4 to 12Hz (Supplementary materials Figures S1-S2 for detailed information and process results of data processing).

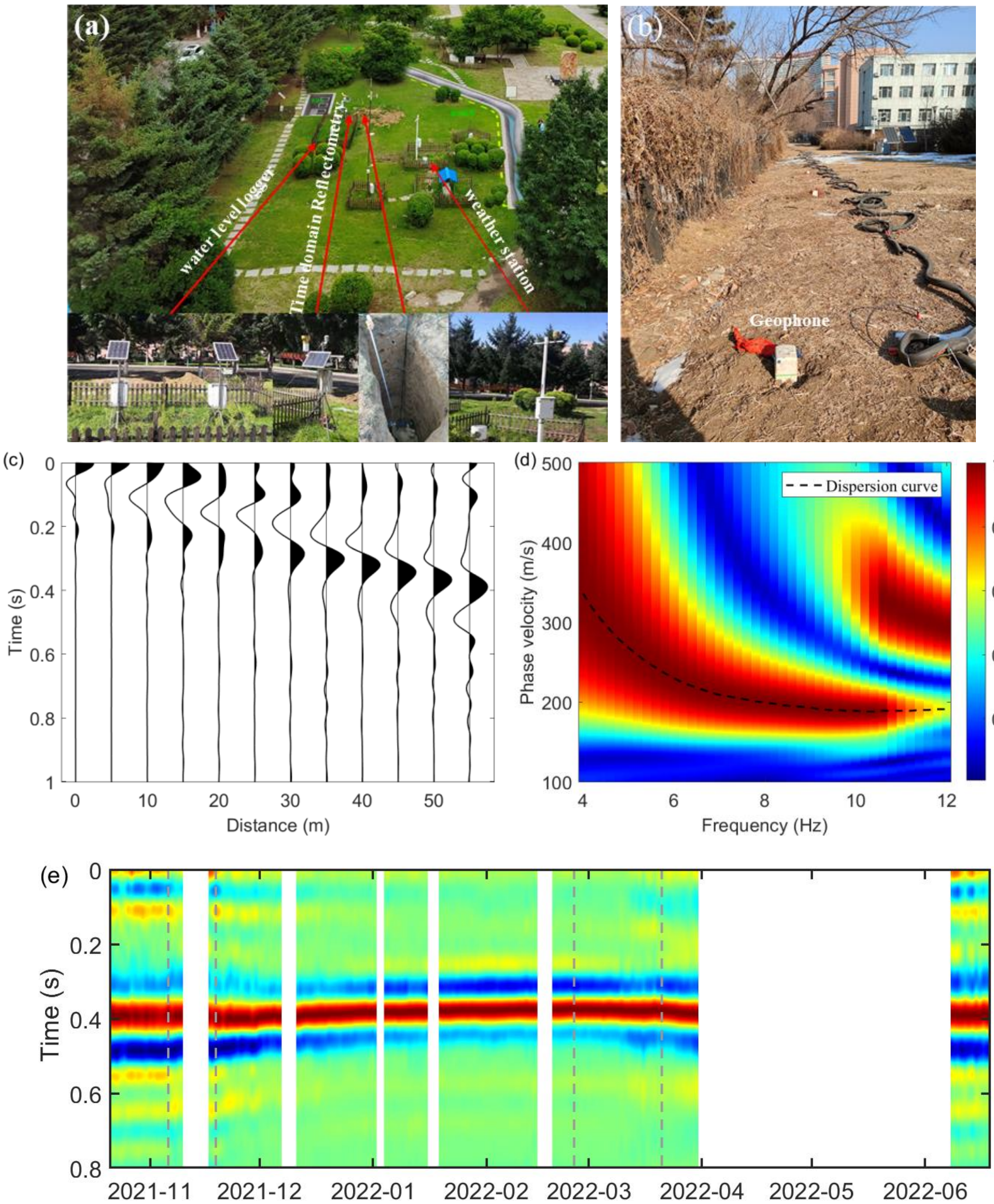

Figure 1. Experiment site and NCF data overview. (a) Map of the experiment with various hydrological data acquisition; (b)Map of the seismic node array; (c) Noise cross-correlation function; (d) The corresponding surface-wave dispersion curve; (e) The time-lapse NCF for the 1st

and 12th station pairs (There was some missing data due to the instrument recharge and the lockdown of the COVID-19 epidemic.).

3. Methods

3.1 Relative Velocity Variations (dv/v)

The NCF calculated by seismic noise interferometry is formed of ballistic waves (body, multi-mode surface waves) and coda waves. Coda waves are preferred to ballistic waves simply because of their long paths that make them more sensitive to small changes of the medium and better robustness to non-ideal noise source distribution (Grêt et al., 2006; Sens-Schoenfelder and Wegler, 2006; Mao et al., 2023). In our work, the seismic wave velocity caused by soil freezing and thawing varies greatly, and the traffic noise can be approximated as an ideal noise source because the survey line is close to and parallel to the road. The ballistic waves mixed with diffracted waves that form the early coda can project the observed temporal perturbations of seismic velocities to specific regions at depth (Mordret et al., 2020).

The time-lapse NCFs of the 1st and 12th stations are shown in Figure 1e. Firstly, we use the trace stretching (TS) method to calculate the dv/v between two stations (Lobkis & Weaver, 2003; Sens-Schönfelder & Wegler, 2006). The TS method calculates the stretching parameter ϵ that maximizes the correlation function $C(\epsilon)$ between the reference $CC_r(t)$ and current waveforms $CC_c(t)$ within a selected time window t_2:

$$C(\epsilon) = \frac{\int_{t_1}^{t_2} CC_{c,\epsilon}(t) CC_r(t) dt}{\sqrt{\int_{t_1}^{t_2} (CC_{c,\epsilon}(t))^2 dt} \sqrt{\int_{t_1}^{t_2} (CC_r(t))^2 dt}} \#(1)$$

Where $CC_{c,\epsilon}(t) = CC_c\big(t(1+\epsilon)\big)$, is the waveform of $CC_c(t)$ after stretching, there is a negative correlation between speed variation and stretch parameter ϵ ($dv/v = -dt/t = -\epsilon$). Yuan et al. (2021) proposed a wavelet transform stretching (WTS) method combining continuous wavelet transform (CWT) with TS. It transforms the signal into the wavelet domain by wavelet transform, then intercepts it at a certain frequency or bandwidth. Finally, we use the inverse wavelet to transform the signal into the time domain and measure the relative velocity variation by the TS method. The wavelet transforms, and their reconstruction of specific frequencies or frequency bands are equivalent to the frequency filter in signal processing, which gives the TS method a frequency resolution and provides valuable information to infer the depth of the velocity variations.

3.2 Relative Surface-wave Dispersion Curve Variations (dc/c)

The multichannel analysis of surface waves (MASW) method is one of the primary methods for obtaining shallow dispersion curves (Park et al., 1999). It is widely used in near-surface geophysics and geoengineering due to its non-invasive, non-destructive, efficient, and low-cost characteristics (Xia et al., 2015). The dispersion spectrums of the NCFs were calculated by the linear Radon transform (LRT) (Luo et al., 2008), and the fundamental dispersion curves were picked based on the peak energy of the dispersive spectrums (Figure 1d). We processed daily NCF recordings to obtain the time-lapse phase velocity variations. The following equation calculates the relative surface-wave dispersion curve variations (dc/c):

$$dc/c = \frac{c_c(\omega) - c_r(\omega)}{c_r(\omega)} \tag{2}$$

Where $c_c(\omega)$ and $c_r(\omega)$ are the current and reference dispersion curves, the dispersion curves can be used to invert the time-lapse frozen ground S-wave velocity structure. We evaluated the sensitivity and noise resistance of dc/c and dv/v in response to the soil freezing and thawing process (Synthetic model test comparison can be found in Supporting Information Figures S3-S8). Compared with dv/v, the dc/c has higher sensitivity to S-velocity changes caused by soil freezing and thawing and is more resistant to noise interference.

3.3 HVSR

The horizontal-to-vertical spectral ratio (HVSR) method was proposed by Nakamura (1989, 1997). It has been described in the abundant scientific literature as an efficient tool to determine the resonant frequency of a 1D sedimentary soft layer. The method uses a three-component seismometer to measure the H/V spectral ratio of ambient noise:

$$\frac{H}{V}(\omega) = \sqrt{\frac{E_1(\omega) + E_2(\omega)}{E_3(\omega)}} \tag{3}$$

E_1 and E_2 are spectral energy in the horizontal direction, *and* E_3 is in the vertical direction.

4. Results

4.1 Comparison of dv/v and dc/c during Freeze-thaw Cycle

Figure 2a shows the subsurface SMC change during soil freezing and thawing. Between 19 November 2021 and 25 February 2022, with the decrease in temperature and the increase in the cumulative freezing days, the frozen layer gradually formed and moved downward, and the SMC in the frozen area decreased. Between 25 February and 21 March 2022, air temperatures oscillated around 0 °C, and the downward development of the freeze layer slowed and stabilized. After 21 March, the frozen layer thawed in both directions, downward from the surface and upward from the depth, increasing soil moisture content and returning to pre-freeze soil levels by the end of April. Figures 2b and 2c show the calculated time-lapse dv/v by WTS and the dc/c profiles. The increases in dv/v and dc/c are in agreement with the decrease in SMC, and these processes are associated with decreasing temperatures and soil freezing during the winter of 2021. Compared with the dv/v, dc/c is more consistent with the range of SMC variation boundary (black dashed line).

Figure 2d shows the comparison of the dv/v (blue line) and dc/c (green line) at 12 Hz and SMC at 0 cm depth (red line). The overall trend of dv/v and dc/c fits well. In addition, the curves of dc/c and SMC have a higher negative correlation (vertical gray dashed line), especially in March 2022. We sum up the velocity change from all frequencies to obtain the comparison between the velocity variation and air temperature (Figure 2e). Here, the black line is dv/v by the TS method, the blue line is dv/v by the WTS method, the green line is dc/c, and the red line is air temperature curves. The dv/v (WTS) and dc/c (phase velocity) curves are obtained by averaging the velocity variations over frequency. The overall trend of dv/v (WTS) and dv/v (TS) fit better, while dv/v (TS) has a certain degree of error. It is also easy to understand, as the WTS and dc/c have similar depth information, but there is a slight difference in velocity variations. The dc/c shows more sudden jumps, and some of the jumps agree with the sudden drop in temperature (vertical dashed line). The dv/v is the velocity difference between two stations; the dc/c obtained by a 1D linear array (12 stations in our work) is more consistent with the SMC and can capture more temperature drop events, which has a higher time resolution. This conclusion has also been confirmed in the above model testing. There is a time delay between the minimum air temperature recordings and the maximum velocity variations due to the thermo-elastic strain at the shallow subsurface (Tsai, 2011; Zhang et al., 2023).

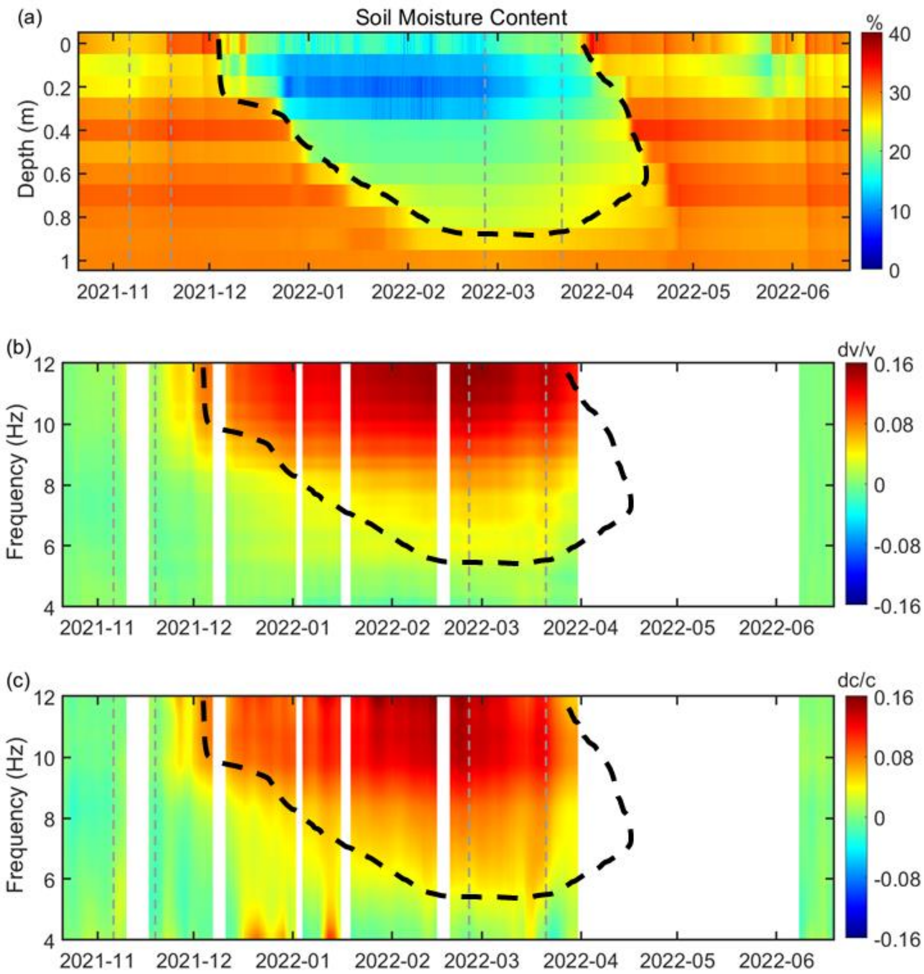

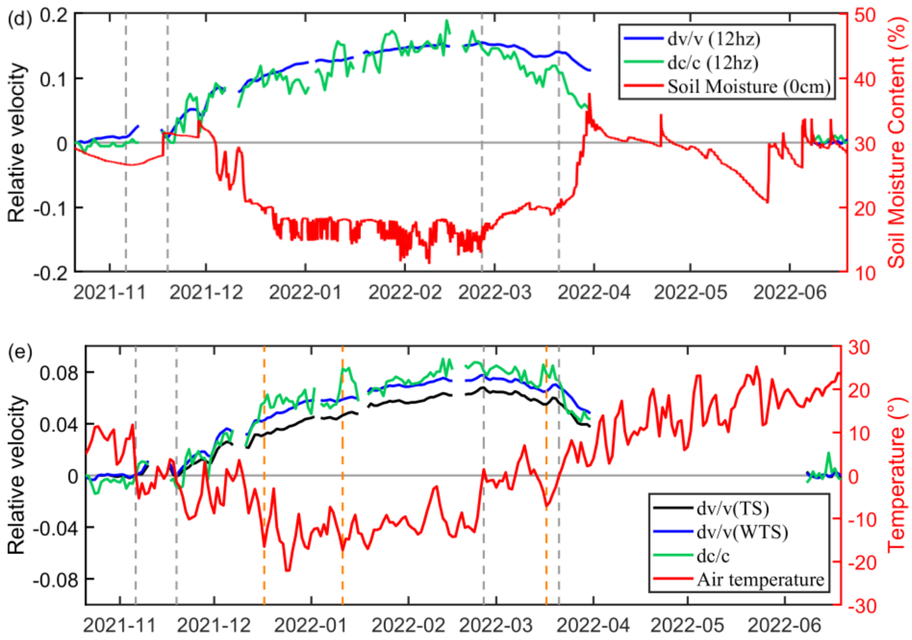

Figure 2. (a) Soil moisture content (black dashed line indicates the variation range of soil moisture content.); (b) Relative velocity variations (dv/v) measured with WTS; (c) Relative phase velocity variations (dc/c); (d) Comparison of dv/v, dc/c and soil moisture content at surface; (e) Comparison of dv/v, dc/c and air temperature.

4.2 Comparison of dc/c, Cumulative Freezing Degree Days, and Groundwater Depth

Figure 3 shows the comparison of dc/c (black line), cumulative freezing degree days (blue line), and groundwater table depth (red line), where S is the cumulative freezing degree days, representing the sum of the average daily temperatures below 0°C over some time (Miao et al., 2019). The dc/c is positively correlated with $\sqrt{|S|}$ between 6 November 2021 and 21 March 2022 and decreases rapidly with the average daily temperature higher than 0°C after 21 March 2022.

During the unfrozen period, there is a positive correlation between groundwater level (red line) and precipitation (bar chart), which verifies the validity of groundwater level data. There were several small increases in the groundwater table on 17 November 2021, 24 May 2022, and 4 June 2022 due to precipitation recharging the groundwater. In the frozen period, the lack of groundwater caused the water table to drop from 21 November 2021 to 27 February 2022. The gradual thawing of snow and frozen soil resulted in the groundwater table rebound after 27 February 2022. There is a strong negative correlation between dc/c and the groundwater depth. The dc/c variation comprehensively affects soil structure, temperature, and groundwater level changes during the freeze-thaw cycle. The groundwater level has low time resolution, and the local variation characteristics of dc/c indicate the variation characteristics of other environmental factors (daily temperature variation).

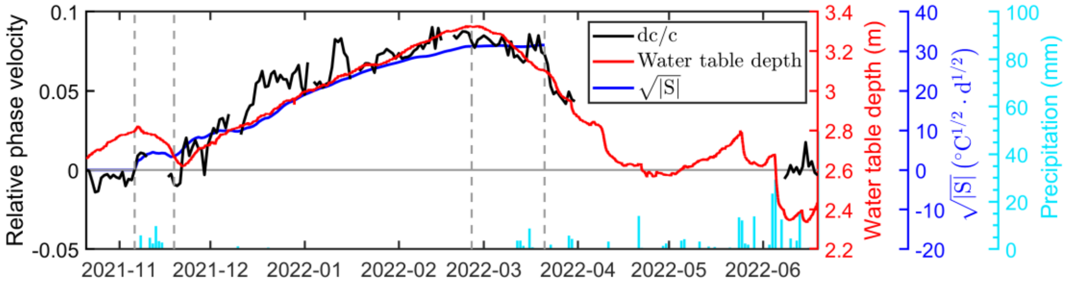

Figure 3. Comparison of dc/c, cumulative freezing degree days, and groundwater table depth.

4.3 HVSR and Attenuation Peak Frequency Variations

The horizontal-to-vertical-spectral-ratio (HVSR) method was used to analyze the difference between the horizontal and vertical components during soil freezing and thawing (Figure 4a). The seismic wavefield experiences an energy decrease during ground freeze with a discrepancy between horizontal and vertical components. The HSVR ratio shows a clear broadband high-frequent decrease at the beginning of December 2021 and the end of April 2022 (Figure 4a). The previous work confirmed that ground frost can cause a broadband decrease in the HVSR for higher frequencies (Guéguen et al., 2017). Our results also suggest that the freezing and thawing of the ground have an impact on the seismic signal. The broadband decrease in the ratio becomes more robust with increasing time or amplitude of the freezing air temperature.

The time-shifted HVSR is averaged in the frequency domain to obtain the time-shifted HVSR mean amplitude curve (red line in Figure 4b). The overall trend of the HVSR curve is consistent with that of the dc/c variations (black line). The unique feature is that the peak inflection point of the HVSR curve is consistent with the minimum air temperature in time, while the dc/c has a time delay mentioned in Figure 2e. When the air temperature reaches its lowest point, it will cause a sudden change in soil medium properties, such as SMC or soil velocity. Models based on the diffusive field assumption confirm the HVSR can reveal the due to a thin layer of ground frost.

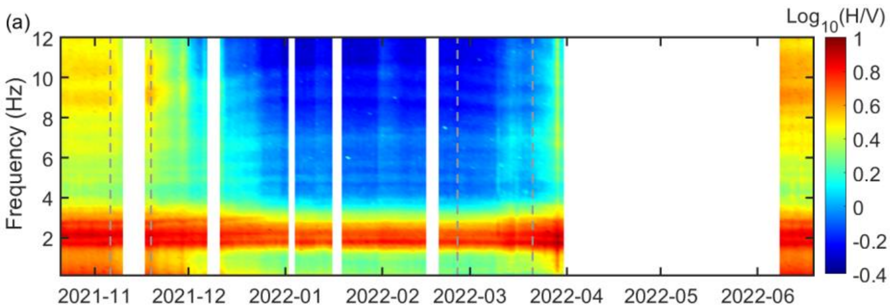

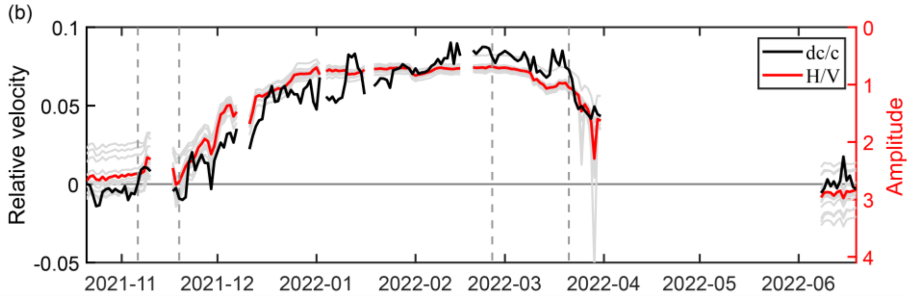

Figure 4. (a) Horizontal-to-vertical spectral ratio of the 6th station; (b) Comparison of dc/c and HVSR (The gray line indicates that the HVSRs of all 12 stations are averaged in the frequency domain, and the red line is the average of the gray lines).

Besides velocity variations, the seismic attenuation during the freezing and thawing cycles is used to evaluate the changes in soil structure and properties.

The quality factor Q provides an effective index for representing the attenuation of seismic wave energy. The lower Q value corresponds to the higher wave energy loss. However, we must measure the seismic amplitude differences and estimate the seismic attenuation coefficient (Zhao et al., 2023). It is difficult to obtain reliable amplitude information in ambient noise data processing. The peak frequency of seismic signals is an alternative characteristic information that characterizes attenuation (Quan et al., 1997). At the same offset seismic data, the peak frequency with attenuation is lower than the seismic signal without attenuation (Li et al., 2017). We calculate the time shift variation of the NCF peak frequency at different offset distances (Figure 5a).

Firstly, the result demonstrates that the larger the offset, the higher the peak frequency, which verifies the reliability of the processed data. Then, during the freezing period, the SMC decreases, and the increase in ice content weakens the soil attenuation, resulting in a higher peak frequency under the same offset distance conditions. Our results are consistent with the basic law of seismic wave attenuation in soil structures (Remy, et al., 1994). In addition, the peak-frequency time shift curve is obtained by averaging the peak frequencies at different offset distances (Figure 5b). The peak frequency gradually increases as the temperature decreases between 6 November 2021 and 27 February 2021 and gradually decreases after 27 February 2022, consistent with the dc/c results. The local abrupt changes in peak frequency especially have a good negative correlation with dc/c and a consistent positive correlation with air temperature, which indicates that the attenuation peak frequency can also provide high sensitivity to near-surface seasonal changes.

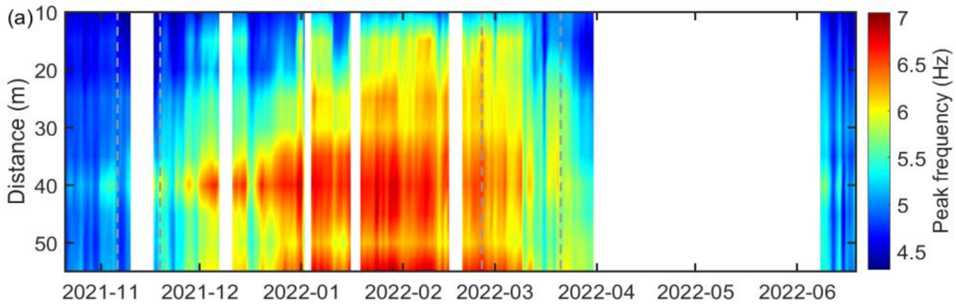

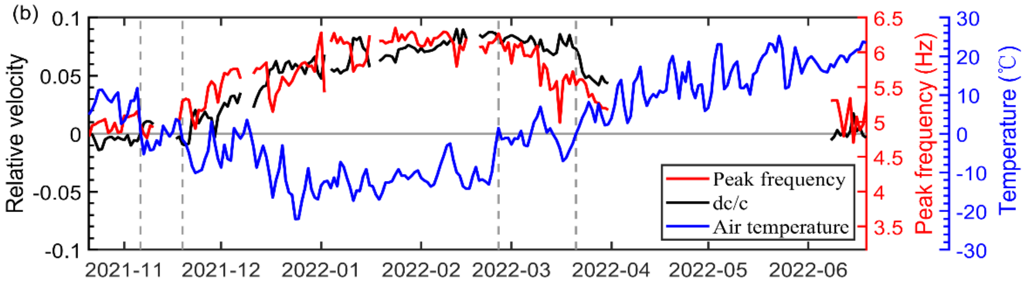

Figure 5. (a) Peak frequency variations; (b) Comparison of relative dc/c and peak frequency variations (The black line indicates that peak frequency averaged in the space domain).

4.4 Time-lapse S-wave Velocity Structure

We used the surface-wave dispersion curve inversion to invert the time-lapse S-velocity model (Figure 6a), where a high-velocity layer (HVL, Vs.>220 m/s) appears on the surface between November 2021 and April 2022. In November 2021, the temperature decreased to below 0 ℃, the surface soil froze, and an HVL appeared. The inverted HVL's maximum thickness is consistent with the frozen ground depth recorded by the hydrological sensor (0.8m). As the temperature increases, the thickness of HVL gradually decreases. After March 2022, the temperature increased to 0 ℃, the frozen soil thawed, and the high-velocity layer gradually disappeared. The quality evaluation (the time-lapse observed and predicted dispersion curves) of inverted results can be found in Figure S9 in Supporting Information.

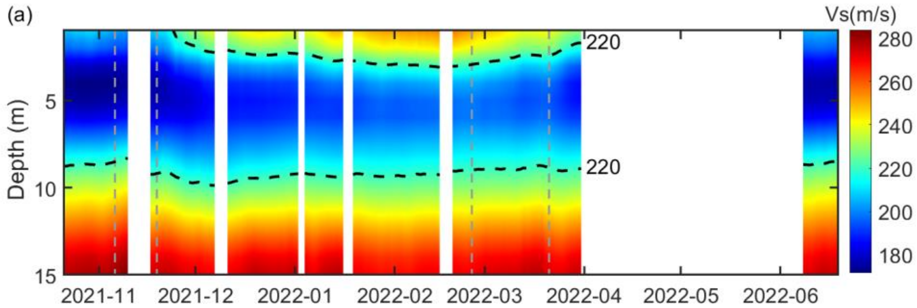

Figure 6. Time-lapse S-wave velocity models constructed from 1D dispersion curve inversion.

5. Discussion

This work combines the 1D linear array of three-component seismic nodes and hydrological sensors to conduct a seasonal frozen freeze-thaw monitoring experiment. The comparison of dc/c and dv/v indicates that the dc/c are more consistent with the SMC and can capture the air temperature drop events (Figure 2). One critical explanation is that the dv/v obtained by the single or two station signals while the dc/c (phase velocity variation) obtained by all 12 station signals can capture more tiny anomalies.

Air temperature below 0℃ causes the subsurface to freeze, increasing the rigidity at the surface and the shear wave velocity (Zimmerman & King, 1986). Between 6 November 2021 and 31 March 2022, when the air temperature is below 0 ℃, and the soil velocity increases, and when the air temperature is above 0 ℃, the soil thaws and relative velocity-variations (dv/v) decreases (Figure 2e). This result suggests that air temperature and dv/v are not linear or delayed. A comparison of $\sqrt{|S|}$ and relative velocity (Figure 3) indicates that dv/v and the cumulative freezing degree days were closely related.

Figure 3 shows the high correlation between dc/c and the groundwater table depth during seasonal freezing and thawing. The results are intrinsically related, and previous studies have shown an anti-correlation between the groundwater table level and dv/v, which is related to saturation, pore pressure, and microstructural (Mao et al., 2022). A rise in the groundwater table causes an increase in water saturation and pore pressure, which prevents the closing of cracks and grain contacts, thereby reducing the velocities. It suggests that dc/c can be a noninvasive method to indicate groundwater level variations during soil freezing and thawing.

In addition to the velocity variations, other seismic data information, such as HVSR and attenuation peak frequency, also show similar changes to dc/c during seasonal freezing and thawing (Figure 4 and Figure 5), which was also confirmed in the previous studies (Guéguen et al., 2017; René Steinmann et al., 2022; Zhao et al., 2023). We tested different S-wave models to simulate the HVSR of frozen and non-frozen soils in Figure S2 (supporting information S1). The results showed that frozen soils lead to a decrease in HVSR, and this increases with increasing frequency. In addition, soil freezing in winter decreases soil moisture content and groundwater table depth, reducing seismic attenuation (Zhao et al., 2023). The peak frequency increases with the increase of quality factor Q. This also validates the reliability of our observations.

Based on the above results, we divided the freeze-thaw process of seasonally frozen ground into four stages (Figure 7). The first stage is the unstable freezing period (I - II), from 6 November 2021 to 19 November 2021, during which the temperature fluctuates around 0°C, and the cumulative freezing degree days increase slowly. The surface soil experienced brief freezing followed by rapid thawing; the relative velocity briefly increased with the effect of soil freezing and thawing and then recovered, and the groundwater table of the unfrozen area increased by rainfall.

The second stage is the stable freezing period (II-III), from 19 November 2021 to 25 February 2022, during which the temperature continued to drop below 0°C, and the negative accumulation temperature continued to increase. The soil temperature decreased to the freezing temperature of soil water, and some of the liquid water in the soil underwent a phase change, resulting in soil freezing, an increase in ice content in the soil freezing layer, and a decrease in unfrozen water content, and a decrease in matrix potential. Under the effect of the matrix potential gradient, the water in the unfrozen area of the soil continuously migrated to the freezing front (cyan curves with arrows), increasing soil freezing depth and the rapid decrease in the groundwater table. In this process, the upward migration of salt with water may aggravate the process of soil salinization. The relative velocity increased rapidly under soil freezing, and HVSR decreased with the increase in velocity. In addition, soil freezing also decreases moisture content and groundwater table depth, reducing seismic attenuation and increasing peak frequency.

The third stage is the unstable thawing period (III-IV), which lasted from 25 February to 21 March 2022, during which the temperature rebounded to near 0°C, and the negative accumulation temperature became smooth. The frozen water in the soil freeze layer began to thaw slowly, the water content increased slowly, and the liquid water migrated from the thaw front to the lower part of the soil layer under the influence of the gravity potential gradient (blue curves with arrows), causing in the groundwater table to rebound. The relative velocity decreased slowly due to the effect of soil thawing, and HVSR increased with the decrease in velocity. In addition, soil thawing also increases moisture content and groundwater table depth, increasing the seismic attenuation and decreasing the peak frequency.

The fourth stage is the stable thawing period (IV -), from 21 March to the end of April 2022. During this period, the temperature increased above 0°C. As the air temperature and surface temperature increased, the frozen ground entered the rapid thawing stage, and the surface soil showed a 'two-way' thawing phenomenon from the surface downward and from the bottom upward. This stage is similar to the previous one, with accelerated relative velocity, HVSR, and peak frequency variation rate.

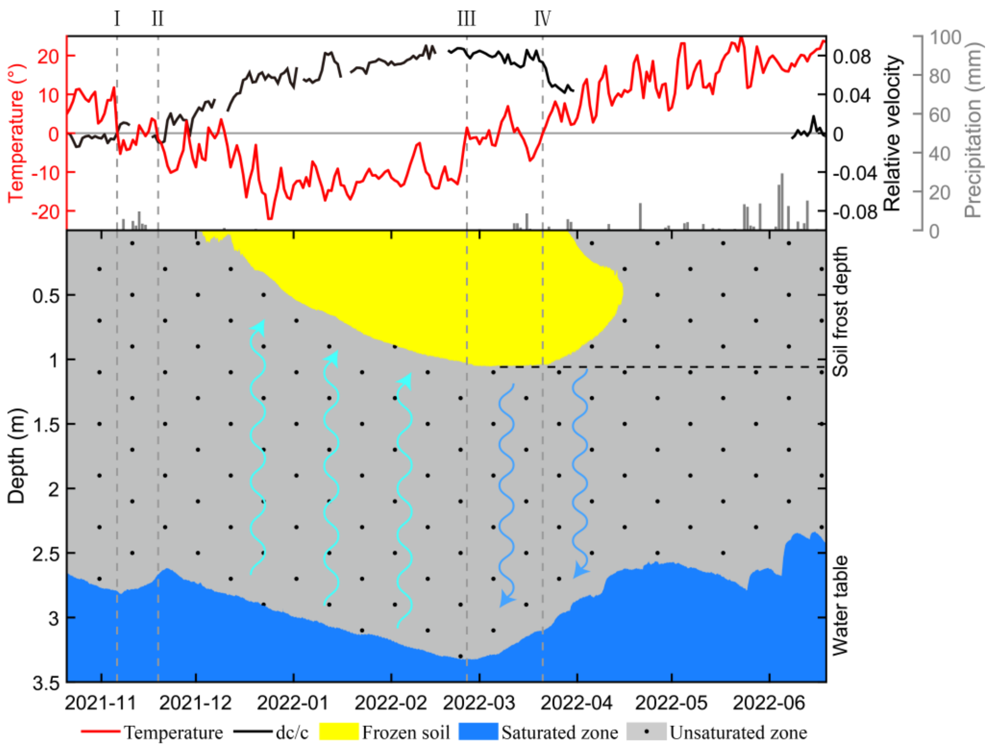

Figure 7. Depicts a schematic representation of the seasonal frozen ground freeze-thaw process (The cyan and blue curves with arrows show the water movement paths)

6. Conclusions

In this paper, we processed ambient seismic noise data from a 1D linear array and compared it with hydrological monitoring data. The results show that seasonal frozen ground freeze-thaw processes cause variations in relative velocity (dv/v and dc/c), HVSR, and peak frequency at shallow ground surfaces. Compared with the dv/v measured by the coda or ballistic waves, the dc/c obtained by multichannel is more consistent with the variation of SMC and captures some temperature drop events. The dc/c and the cumulative freezing degree days were closely related and can indicate variations in the groundwater table during soil freezing and thawing. The peak frequency of NCF at different offsets increases, and a broadband decrease in the time-lapse HVSR is highly correlated with dc/c during winter. The field data experiment demonstrates the effectiveness of ambient noise seismic methodology in detecting near-surface velocity variations and quantitatively monitoring seasonal frozen ground freeze-thaw processes.

Data Availability Statement

To facilitate open research, the data used in this manuscript are available to the public. This includes the part of raw seismic data and the hydrological monitoring data of the experimental site (available on https://zenodo.org/records/10565918). The reviewers as well as the editor may request access during the review stage of this manuscript.

Acknowledgements

The authors want to thank everyone involved in the field campaign and the discussion of the results. Especially, we want to thank Prof. Jianghai Xia, Prof. Haijiang Zhang for constructive discussions about seismic data process. These works are supported by the Natural Science Foundation of China (42222407 and 42174065)

Reference

Albaric, J., Kühn, D., Ohrnberger, M., Langet, N., Harris, D., Polom, U., et al. (2021). Seismic monitoring of permafrost in Svalbard, Arctic Norway. *Seismological Research Letters*, 92(5), 2891–2904. https://doi.org/10.1785/0220200470

Bensen, G. D., Ritzwoller, M. H., Barmin, M. P., Levshin, A. L., Lin, F., Moschetti, M. P., et al. (2007). Processing seismic ambient noise data to obtain reliable broadband surface wave dispersion measurements. *Geophysical Journal International*, 169(3), 1239-1260.

Cheng, G., & Wu, T. (2007). Responses of permafrost to climate change and their environmental significance, Qinghai-Tibet Plateau. *Journal of Geophysical Research: Earth Surface*, 112(F2). https://doi.org/10.1029/2006JF000631

Cheng, F., Lindsey, N. J., Sobolevskaia, V., Dou, S., Freifeld, B., Wood, T., et al. (2022). Watching the cryosphere thaw: Seismic monitoring of permafrost degradation using distributed acoustic sensing during a controlled heating experiment. *Geophysical Research Letters*, 49, e2021GL097195. https://doi.org/10.1029/2021GL097195

Frauenfeld, O. W., & Zhang, T. (2011). An observational 71-year history of seasonally frozen ground changes in the Eurasian high latitudes. *Environmental Research Letters*, 6(4), 044024. https://doi.org/10.1088/1748-9326/6/4/044024

Grêt, A., Snieder, R., & Scales, J. (2006). Time-lapse monitoring of rock properties with coda wave interferometry. *Journal of Geophysical Research: Solid Earth*, 111(B3).

Guéguen, P., Langlais, M., Garambois, S., Voisin, C., & Douste-Bacqué, I. (2017). How sensitive are site effects and building response to extreme cold temperature? The case of the Grenoble's (France) City Hall building. *Bulletin of Earthquake Engineering*, 15(3), 889–906. https://doi.org/10.1007/s10518-016-9995-3

Green, J. K., Seneviratne, S. I., Berg, A. M., Findell, K. L., Hagemann, S., Lawrence, D. M., & Gentine, P. (2019). Large influence of soil moisture on long-term terrestrial carbon uptake. *Nature*, 565(7740), 476– 479. https://doi.org/10.1038/s41586-018-0848-x

Hornum, M. T., Betlem, P., & Hodson, A. (2021). Groundwater flow through continuous permafrost along geological boundary revealed by electrical resistivity tomography. *Geophysical Research Letters*, 48, e2021GL092757. https://doi.org/10.1029/2021GL092757

Harris, C., Arenson, L. U., Christiansen, H. H., Etzelmüller, B., Frauenfelder, R., Gruber, S., et al. (2009). Permafrost and climate in Europe: Monitoring and modelling thermal, geomorphological and geotechnical responses. *Earth-Science Reviews*, 92(3-4), 117–171. https://doi.org/10.1016/j.earscirev.2008.12.002

Jorgenson, M. T., Racine, C. H., Walters, J. C., & Osterkamp, T. E. (2001). Permafrost degradation and ecological changes associated with a warming climate in central Alaska. *Climatic change*, 48(4), 551-579.

James, S. R., Knox, H. A., Abbott, R. E., Panning, M. P., & Screaton, E. J. (2019). Insights into permafrost and seasonal active-layer dynamics from ambient seismic noise monitoring. *Journal of Geophysical Research: Earth Surface*, 124, 1798– 1816. https://doi.org/10.1029/2019JF005051

Kula, D., Olszewska, D., Dobiński, W., & Glazer, M. (2018). Horizontal-to-vertical spectral ratio variability in the presence of permafrost. *Geophysical Journal International*, 214(1), 219–231. https://doi.org/10.1093/gji/ggy118

Li, J., Dutta, G., & Schuster, G. (2017). Wave-equation Qs inversion of skeletonized surface waves. *Geophysical Journal International*, 209(2), 979-991. https://doi.org/10.1093/gji/ggx051

Lindner, F., Wassermann, J., & Igel, H. (2021). Seasonal freeze-thaw cycles and permafrost degradation on Mt. Zugspitze (German/Austrian Alps) revealed by single-station seismic monitoring. *Geophysical Research Letters*, 48, e2021GL094659. https://doi.org/10.1029/2021GL094659

Lobkis, O. I., & Weaver, R. L. (2003). Coda-wave interferometry in finite solids: Recovery of P-to-S conversion rates in an elastodynamic billiard. *Physical review letters*, 90(25), 254302.

Luo, Y., Xia, J., Miller, R. D., Xu, Y., Liu, J., & Liu, Q. (2008). Rayleigh-wave dispersive energy imaging using a high-resolution linear Radon transform. *Pure and Applied Geophysics*, 165, 903-922.

Miao, Y., Shi, Y., Zhuang, H. Y., Wang, S. Y., Liu, H. B., & Yu, X. B. (2019). Influence of seasonal frozen soil on near-surface shear wave velocity in eastern Hokkaido, Japan. *Geophysical Research Letters*, 46, 9497– 9508.

https://doi.org/10.1029/2019GL082282

Mollaret, C., Hilbich, C., Pellet, C., Flores-Orozco, A., Delaloye, R., & Hauck, C. (2019). Mountain permafrost degradation documented through a network of permanent electrical resistivity tomography sites. *The Cryosphere*, 13(10), 2557–2578. https://doi.org/10.5194/tc-13-2557-2019

Mordret, A., Courbis, R., Brenguier, F., Chmiel, M., Garambois, S., Mao, S., ... & Hollis, D. (2020). Noise-based ballistic wave passive seismic monitoring–Part 2: surface waves. *Geophysical Journal International*, 221(1), 692-705.

Mao, S., Lecointre, A., van der Hilst, R. D., & Campillo, M. (2022). Space-time monitoring of groundwater fluctuations with passive seismic interferometry. *Nature communications*, 13(1), 4643.

Mao, S., Ellsworth, W. L., & Beroza, G. C. (2023). Adaptive Coda-Wave Imaging With Voronoi Tessellation. *Journal of Geophysical Research: Solid Earth*, 128(8), e2023JB026592.

Nakamura, Y., (1989). A method for dynamic characteristics estimation of subsurface using microtremor on the ground surface, Q. Rep. Railw. *Tech. Res. Inst*., 30(1), 25–33.

Nakamura, Y. (1997). Seismic vulnerability indices for ground and structures using microtremor. In World congress on railway research in Florence, Italy.

Niu, L., Ye, B., Li, J., & Sheng, Y. (2011). Effect of permafrost degradation on hydrological processes in typical basins with various permafrost coverage in Western China. *Science China Earth Sciences*, 54, 615-624. https://doi.org/10.1007/s11430-010-4073-1

Nelson, F. E. (2003), (Un)frozen in time, Science, 299, 1673 – 1675.

Remy, J-M., Bellanger, M., & Homand-Etienne, F. (1994). Laboratory velocities and attenuation of P-waves in limestones during freeze-thaw cycles. *Geophysics*, 59: 245-251.

Park, C. B., Miller, R. D., & Xia, J. (1999). Multichannel analysis of surface waves. *Geophysics*, 64(3), 800-808.

Qin, Y., Chen, J., Yang, D., & Wang, T. (2018). Estimating seasonally- frozen ground depth from historical climate data and site measurements using a Bayesian model. *Water Resources Research*, 54, 4361-4375.

Qin, L., Steidl, J. H., Qiu, H., Nakata, N., & Ben-Zion, Y. (2022). Monitoring seasonal shear wave velocity changes in the top 6 m at Garner Valley in southern California with borehole data. Geophysical Research Letters, 49, e2022GL101189.

Quan, Y., & Harris, J. M. (1997). Seismic attenuation tomography using the frequency shift method. *Geophysics*, 62(3), 895-905.

Schimmel, M., & Gallart, J. (2007). Frequency-dependent phase coherence for noise suppression in seismic array data. *Journal of Geophysical Research: Solid Earth*, 112(B4).

Stemland, H., Johansen, T., Ruud, B., & Romeyn, R. (2021). Active versus passive seismic monitoring of near-surface arctic thawing. Nsg2021 2nd conference on geophysics for infrastructure planning, monitoring and BIM, 2021, 1–5. https://doi.org/10.3997/2214-4609.202120071

Scandroglio, R., Draebing, D., Offer, M., & Krautblatter, M. (2021). 4D quantification of alpine permafrost degradation in steep rock walls using a laboratory-calibrated electrical resistivity tomography approach. *Near Surface Geophysics*, 19(2), 241–260. https://doi.org/10.1002/nsg.12149

Sobolevskaia, V., Ajo-Franklin, J., Cheng, F., Dou, S., Lindsey, N., & Wagner, A. (2021). Tracking surficial aquifer state using DAS and ballistic Rayleigh waves. *SEG Technical Program Expanded Abstracts*: 1942-1946. https://doi.org/10.1190/segam2021-3583758.1

Steinmann, R., Seydoux, L., & Campillo, M. (2022). AI-based unmixing of medium and source signatures from seismograms: Ground freezing patterns. *Geophysical Research Letters*, 49, e2022GL098854. https://doi.org/10.1029/2022GL098854

Sens-Schönfelder, C. & Wegler, U., (2006). Passive image interferometry and seasonal variations of seismic velocities at Merapi V olcano, Indonesia, *Geophys. Res. Lett.*, 33(21). https://doi.org/10.1029/2006GL027797

Tsai, V. C. (2011). A model for seasonal changes in GPS positions and seismic wave speeds due to thermoelastic and hydrologic variations. *Journal of Geophysical Research*, 116(B4), B04404. https://doi.org/10.1029/2010JB008156

Vecellio, D. J., Nowotarski, C. J., & Frauenfeld, O. W. (2019). The Role of Permafrost in Eurasian Land-Atmosphere Interactions. *Journal of Geophysical Research: Atmospheres*, 124, 11,644– 11,660. https://doi.org/10.1029/2019JD031204

Wang, Q.-Y., Brenguier, F., Campillo, M., Lecointre, A., Takeda, T., & Aoki, Y. (2017). Seasonal crustal seismic velocity changes throughout Japan. *Journal of Geophysical Research: Solid Earth*, 122, 7987–8002. https://doi.org/10.1002/2017JB014307

Walvoord, M. A., & Kurylyk, B. L. (2016). Hydrologic impacts of thawing permafrost—A review. *Vadose Zone Journal,* 15(6), vzj2016.01.0010. https://doi.org/10.2136/vzj2016.01.0010

Xia, J. H., Gao, L. L., Pan, Y. D., Shen, C., & YIN, X. F. (2015). New findings in high-frequency surface wave method. *Chinese Journal of Geophysics*, 58(8), 2591-2605.

Yuan, C., Bryan, J., & Denolle, M. (2021). Numerical comparison of time-, frequency-and wavelet-domain methods for coda wave interferometry. *Geophysical Journal International*, 226(2), 828-846.

Zimmerman, R., & King, M. (1986). The effect of the extent of freezing on seismic velocities in unconsolidated permafrost. *Geophysics*, 51(6), 1285–1290. https://doi.org/10.1190/1.1442181

Zhang, T., Osterkamp, T. E., & Stamnes, K. (1997). Effects of climate on the active layer and permafrost on the North Slope of Alaska, USA. *Permafrost and Periglacial Processes*, 8(1), 45-67.

Zhang, S., Luo, B., Ben-Zion, Y., Lumley, D. E., & Zhu, H. (2023). Monitoring terrestrial water storage, drought and seasonal changes in central Oklahoma with

ambient seismic noise. Geophysical Research Letters, 50, e2023GL103419.
Zhao, Y., Nilot, E. A., Li, B., Fang, G., Luo, W., & Li, Y. E. (2023). Seismic attenuation extraction from traffic signals recorded by a single seismic station. *Geophysical Research Letters*, 50, e2022GL100548. https://doi.org/10.1029/2022GL100548